Modulation of Stem Cell Adipogenic Differentiation in Response to Mechano-Topographical Factors

BY

HAMED NAIMIPOUR
B.S., University of Illinois at Chicago, Chicago, 2008

THESIS

Submitted as partial fulfillment of the requirements
for the degree of Master of Science in Bioengineering
in the Graduate College of the
University of Illinois at Chicago, 2012

Chicago, Illinois

Defense Committee:
Michael Cho, Chair and Advisor
Shan Sun
Satish Alapati, Endodontics

ACKNOWLEDGEMENTS

I would like to thank my advisor Dr. Michael Cho for his encouragement and support throughout this project. I am grateful to my thesis committee, Dr. Shan Sun, and Dr. Satish Alapati for their insight and perspective throughout this project. I acknowledge Dr. Shan Sun and Dr. Igor Titushkin for being great mentors in helping me develop strategies.

Many thanks to the UIC Nanotechnology Core Facility, particularly Bob Lajos for his technical assistance during this project. I would like to thank Dr. David Eddington for the use of his laboratory equipment and Elizabeth Ferraz for her assistance.

Last, and certainly not least, I would like to thank my family, particularly my father for his confidence in my ability to persist through the worst of times and for believing in me throughout my academic career. He has provided motivation and wisdom for which I am eternally grateful.

HN

TABLE OF CONTENTS

TABLE OF CONTENTS (CONTINUED)

LIST OF ABBREVIATIONS

AFM	Atomic Force Microscopy
αMEM	Alpha-Modified Eagle's Medium
BSA	Bovine Serum Albumin
DAPI	4',6-diamidino-2-phenylindole
ECM	Extracellular Matrix
FBS	Fetal Bovine Serum
HBSS	Hanks Buffered Salt Solution
hMSCs	Human Mesenchymal Stem Cells
PDMS	Polydimethylsiloxane
DIC	Differential Interface Contrast
TRITC	Tetramethylrhodamine Isothiocyanate
HCL	Hydrochloric Acid
CAD	Computer Aided Design
Cr	Chromium
DNA	Deoxyribonucleic Acid
PBS	Phosphate Bufferred Saline
PGA	Poly(glycolic acid)
PLA	Poly(lactic acid)
PLGA	Poly(lactic-co-glycolic acid)
PLLA	Polylactide
SiOH	Silanol
STM	Scanning Tunneling Microscope

LIST OF FIGURES

LIST OF FIGURES (CONTINUED)

FIGURE PAGE

LIST OF FIGURES (CONTINUED)

FIGURE PAGE

SUMMARY

Regenerative medicine seeks to present a healing or therapeutic platform by generating or controlling the microenvironmental niche in order to dictate stem cells differentiation into the desired cell types and ultimately guide tissue development. Stem cells possess the ability to self-renew without limit and are able to differentiate into multiple types of functional cells in response to biophysical and biochemical signals. These defining abilities make it an attractive source of cells for regeneration and repair of damaged or lost tissue. Proliferation and differentiation of stem cells in their in vivo environment is dictated by their surrounding microenvironment known as the stem cell niche. In the last several years, attention has been drawn to the study of the physical microenvironment as increasing evidence suggests that cells are regulated by physical properties of the stem cell niche in addition to soluble factors. Physical properties such as mechanical stiffness and topography of the cell microenvironment have been shown to direct stem cell lineage. However, few studies have investigated such effects on adipogenesis.

This study was designed to evaluate adipogenic differentiation of human mesenchymal stem cells (hMSCs) when introduced to patterned substrata with parameters in the micron and submicron range. In addition the mechanical properties were also varied. Substrata were fabricated using photolithography. Topographical features containing parameters both in the micron and submicron range (posts, height ~ 114 nm) were spaced 200 microns apart in order to encourage aggregate formation of cells. Characterization of substrate stiffness and topographical feature parameters were done using an atomic force microscope. 10:1 base to cross linker silicone substrates (E =2.76 MPa) and 30:1 polymers

(E= 0.26 MPa) were fabricated with and without posts. Patterned substrates Lipid formation was examined by Oil Red O staining followed by quantitative analysis using spectrophotometry. Relative percent lipid area formation was also determined by image analysis. In addition, actin cytoskeleton structure was visualized.

The results indicate that both mechanical and topographical cues may be introduced to manipulate stem cell responses. Oil Red O staining of patterned samples at days 4, 7, and 14 revealed aggregate formation of cells on the posts whereas cells were more evenly distributed on plain silicone surfaces. Percent lipid area formation was higher at days 4 and 7 of differentiation on patterned substrates. Soft patterned substrates showed more lipid formation at early time points. These results suggest that surface topography with parameters in the micron and submicron range may play a significant role in modulation of adipogenic differentiation. The results of this study may assist in the strategic design of in vitro models for soft tissue engineering applications.

I. BACKGROUND

A. Introduction

Soft tissue defects can result from traumatic injuries, burns, congenital defects, chronic diseases and tumor resections. These defects are primarily a result of adipose tissue or fat loss (1). Currently, reconstructive surgery is the common approach for treatment and correction of soft tissue defects. The 2011 plastic surgery statistics report provided by the American Society of Plastic Surgeons states that nearly 5.5 million reconstructive plastic surgeries were performed in the United States alone, with the majority attributed to procedures following tumor removal (2). Nearly 4.2 million (approximately 77%) of reconstructive procedures were attributed to procedures involving tumor removal (3). For example, breast cancer that is the most common form of cancer among women which requires treatments such as lumpectomy or mastectomy. These procedures require reconstruction post surgery. Currently, the common treatment modality for soft tissue defects is the use of autologous grafts or commercially available synthetic filler materials and implants (1). Grafting is often followed by resorption over time due to necrosis of the tissue as a result of insufficient vascularization. Donor site tissue availability and donor site morbidity are also additional limitations that exist. Longevity, escape of particles, immune response to the synthetic implant material is of major concern as well (4).

Tissue engineering methods offer novel strategies and solutions to such limitations in which engineered tissue can be tailored to mimic adipose tissue both structurally and functionally. In addition, the development of *in vitro* adipose tissue test systems can be used towards type 2 diabetes and obesity research.

B. Microenvironmental Milieu and Stem Cell Behavior

Stem cells present great potential as a cell source for use in tissue engineering models due to their two defining characteristics, unlimited self-renewal and their ability to differentiate into multiple cell types or their multi-lineage potential when provided with appropriate stimuli from their surrounding microenvironment. These characteristics are necessary for generation of tissue because all cells including stem cells exist in a natural *in vivo* environment that is comprised of a combination of chemical and physical components (5). As such, an ability to closely mimic the natural microenvironment would be ideal for controlling cell adhesion, growth, and survival. Some important factors of the microenvironment that affect cellular behavior are the physical properties such as stiffness and elasticity, biochemical signals such as growth hormones, and the topography of adhesive sites (6). As an example, adult stem cells have been shown to commit to various lineages based on the stiffness of the matrix to which they are exposed. It has been shown that mesenchymal stem cells plated on substrates with low stiffness expressed brain lineage markers whereas MSCs plated on substrates with high stiffness expressed bone lineage markers (6).

The ability for a cell's environment to influence its orientation, migration, and cytoskeletal organization was first noted in 1911, and the topography of that environment was proposed to be the cause in 1964 (7). The topography of a surface has been shown to influence cell migration, proliferation, morphology, adhesion and differentiation (8). In one study, human mesenchymal stem cells (hMSCs) were shown to exhibit enhanced neuronal differentiation in the presence of nanogratings. hMSCs were cultured on poly(dimethylsiloxane) (PDMS) scaffolds comprised of 350 nm, 1 μm, or 10 μm wide

gratings 350 nm in depth. To increase cell adhesion, all scaffolds were coated in bovine collagen I (9). There are several studies that have investigated the effects of pattern size and geometrical shape of topographical patterns on adipogenic differentiation of stem cells (10).

Cells have an array of tools at their disposal to sense their environment. When such sensors contact the ECM, such as focal adhesions (FA), which serve as a link between the ECM and the cellular cytoskeleton, they can trigger a signal cascade back to the nucleus. Differential attachment patterns as a result of introducing different substrates could result in rearrangement of the actin cytoskeleton, which could trigger an intercellular cascade leading to differentiation of the cells. Another possible pathway could be transmission of signals through integrin receptors on the cell surface, through the cytoskeleton, and into the nucleus. While it has been demonstrated that changes in the microtopography affects cell behavior, the exact process is still largely unknown. Actin cytoskeleton rearrangement has been shown to be altered by stiffness variation of substrates and the presence of topographical features. In this study, the F-actin network of hMSCs plated on substrates containing microtopography was observed.

C. Scaffolds for Soft Tissue Engineering

There have been various types of materials used as possible candidates for soft tissue engineering applications. Both synthetic and natural scaffolds have been fabricated for the purpose of engineering soft tissue constructs with the intention of the material possessing several desired standard qualities such as biocompatibility, biodegradability, ease of sterilization and ability to support cell growth. Synthetic polymers that have been used as

scaffolds include PLLA, PGA, and PLGA. These materials are attractive for tissue engineering purposes as they are biodegradable and have been approved by the FDA for specific *in vivo* applications. The natural materials used have been natural materials of the ECM such as collagen, alginate, and fibrin. In the case of natural materials, collagen sponges and hyaluronic acid gels have been assessed to be potential biomaterials for soft tissue engineering applications (11, 12).

Some limitations associated with synthetic polymers are the necrosis of tissue associated with the high acidic environment generated by the degradation of the material over time. Natural polymers are challenging to work with due to the difficulty that exists with controlling and tailoring design parameters such as porosity, architecture and mechanical stiffness. As a result, there are several natural and synthetic materials that can be used for soft tissue engineering applications. However, in order to successfully develop a cell based implant for tissue engineering purposes, one needs to understand the interaction between cells and the scaffold material and also that of cells with the surrounding tissue.

D. Mesenchymal Stem Cells

Human bone marrow consists of stem-like cells that have been extensively used in the clinical setting due to their ready isolation for autologous use and ability to differentiate along various tissue-specific lineages. These cells act as precursors to non-hematopoietic tissue. These cells are also called plastic-adherent cells because of their strong adhesion to culture plates. They have fibroblast like morphology (13). Human bone marrow is a source of MSCs that are capable of adipogenic, chondrogenic, osteogenic, and neurogenic differentiation and have multi-lineage potential provided with appropriate soluble factors.

Adipocytes develop from multipotent mesenchymal stem cells and the adipogenic potential of hMSCs has been studied both using *in vitro* and in vivo models and have also been shown to have promising clinical results (11, 14).

Similar to embryonic stem cells that have totipotent characteristics, hMSCs have been demonstrated to differentiate along the chondrogenic, osteogenic, myogenic, neurogenic, and adipogenic lineages (15, 16). Human embryonic stem cells have been induced to generate cardiomyocytes, chondrocytes, endothelial cells, and osteoblasts (17). The similar characteristics of hMSCs to embryonic stem cells are attractive to investigators who are debating whether they should use embryonic stem cells or mesenchymal stem cells. In addition to the ethical aspects accompanied with the use of embryonic stem cells, their ability to self renew without limit and differentiate into almost all types of cells provides a major disadvantage. Uncontrolled proliferation and differentiation of these cells has lead to formation of teratomas or cancerous growths (18).

E. Microfabrication

Microfabrication broadly describes fabrication technologies used to make technology and various components on the micron scale or more generally it is defined as fabrication of miniature devices. It involves the rapid fabrication of thousands of identical structures accomplished by techniques such as replica molding, polymer hot embossing, imprinting, photolithography and casting (19). The method used for the purpose of executing this experiment was photolithography. This method offers excellent geometric control, features in the micron scale, submicron range and reproducibility. These highly attractive characteristics of photolithography allows for single cell analysis. The result of such a

method is more biologically significant studies that can be used to produce improved medical devices and biological constructs.

Photolithography is the process of manipulating printed patterns to form a mask that transfers desired light to a light-sensitive photoresist on a substrate (20). The design that is to be etched or generated into the substrate is done using a CAD program and then drawn into a mask. The mask used in the case of the work described here is a transparent 5 inch x 5 inch quartz plate onto which the CAD design is deposited in a thin chrome layer. Masks used in the process of photolithography are either dark field or bright field. In a dark field mask, the patterned area is transparent while the rest is covered with chrome. Conversely, in a bright field mask, the patterned area is deposited with chrome and the rest of the mask field is transparent. A dark field mask was used in this study to produce PDMS or silicone substrates containing posts by executing standard soft lithography protocol.

F. Soft Lithography

Soft lithography is the process of creating a replica of the master mold created using photolithography (21). For biological experiments involving living cells and cell culture, the general approach is to transfer the generated pattern onto a polymer. Silicone or polydimethylsiloxane (PDMS) under the product name of Sylgard 184 is the most common polymer used in soft lithography. It is an inert, non-flammable, and optically transparent polymer (22). However, its major disadvantage is its hydrophobic property once it has cross linked and formed an elastic solid. In brief, PDMS is commercially available and contains two components, the elastomer base component (SYLGARD 184 Silicone Elastomer Base) and a cross linking or curing agent. These two components are thoroughly mixed and cured

until PDMS forms a hydrophobic solid. In the case of soft lithography, this originally liquid polymer can be poured onto the master mold containing the desired micro-patterns and then cured, thereby creating or transferring desired micro-patterns onto PDMS solidified substrates.

There are several ways to at least reduce the hydrophobic nature of solidified PDMS substrates. Plasma oxidation surface treatments have the ability to alter the surface chemistry by temporarily adding silanol groups to the surface making the surface temporarily hydrophilic. This temporary surface chemistry reverts back to the original hydrophobic contact angle quite easily if exposed to air, therefore, the treated surface needs to be covered by a liquid solution. During this time, the surface resists hydrophobic absorption and negative charges. Even under vacuum, the hydrophobicity of the surface will return over a period of time greater than one week (23). PDMS was used in this experiment due to its stable and biocompatible nature. In addition, the material was suitable for creating a substrate to study the effects of topography as well as topographical stiffness on cell function by varying the cross linker to base ratio.

G. Atomic Force Microscopy

An atomic force microscope (AFM) is a type of scanning probe microscope (SPM) which has the capability of revealing information concerning surface properties of materials at the atomic and molecular level. Surface properties of materials of interest can be observed with very accurate resolution ranging from 100 microns to less than 1 micron (24). Three dimensional topographic analyses of surfaces can be obtained with lateral resolution down to 1.5 nm and vertical resolution down to 0.05 nm. Atomic force microscopy is applied to

various types of materials such as metal semiconductors, conductive and nonconductive materials, synthetic and natural polymers, and even biological samples. For this reason, this technique is attractive for many areas of research including material sciences, polymer science, nanotechnology and biotechnology (24).

The atomic force microscope was invented by Gerd Binning et. al. in 1986. This was several years after the Scanning Tunneling Microscope (STM) had been introduced to the scientific community by Binning and Rohrer in 1982 (25). The STM is essentially the ancestor of all scanning probe microscopes and it measures the tunneling current of a surface and therefore can only be used for conducting surfaces. However, the atomic force microscope has the ability to scan nonconductive materials such as biological materials and polymers. Its ability to scan and measure nonconductive materials is due to its dissimilar method of scanning and data collection. An atomic force microscope measures the force acting between a fine sharp tip which comes into contact or in very close proximity to the sample of interest being imaged or indented for mechanical force measurements. The fine tip is generally a few microns long and often less than 100 angstroms in diameter. The tip is attached to a spring in the form of a cantilever and is then brought close to the surface of interest. Attractive and repulsive forces resulting from interaction between the tip and the surface will create positive or negative bending of the cantilever in the z direction. The bending from the cantilever is then detected by a laser beam that is directed on the cantilever and reflected. The reflection is finally detected by a photo diode and translated into an image. Figure 1 shows the basic concept of AFM.

In addition to imaging, force curve measurements can be obtained using an atomic force microscope which can give valuable data regarding elasticity, adhesion, and hardness

of biological (such as cells and tissue samples) and non biological (such as polymer substrates) samples. The amount of force between the cantilever and sample surface is dependent on the spring constant or stiffness of the cantilever and the distance between the probe and the sample surface. In this experiment, force curve measurements were obtained by repeatedly bringing the probe tip close to the PDMS substrate surfaces and retracted. Force curve measurements were used to determine mechanical properties (elasticity) of silicone substrates with varied elasticity. The method of elasticity measurement is explained more in detail in the methods section.

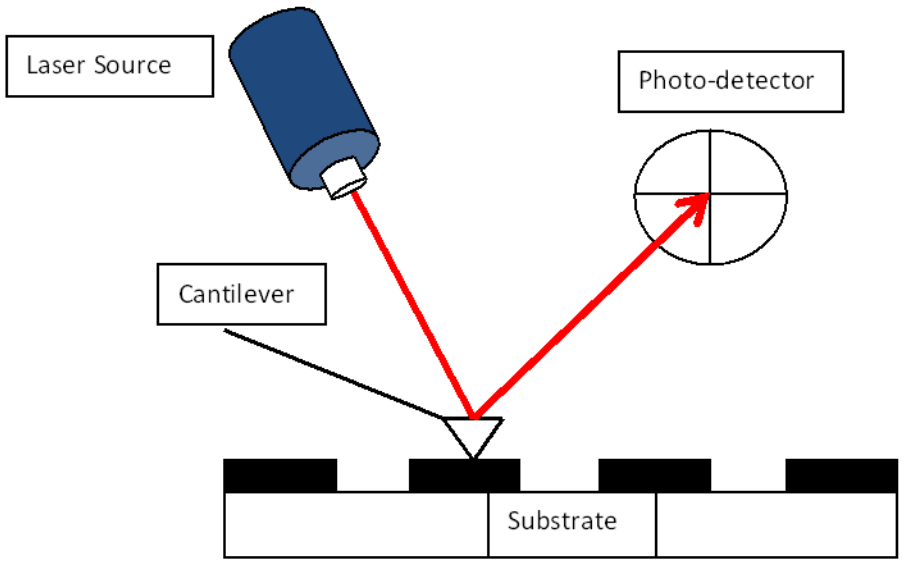

Figure 1. Concept of atomic force microscopy measurement technique where a laser beam is focused and directed on a cantilever, reflected, and detected via a photo diode.

Contact mode AFM, intermittent or tapping mode AFM, and non-contact mode AFM are the three primary imaging modes of atomic force microscopy. In this experiment, contact mode imaging which is the most common method of operation was used for its advantages over other methods. In contact mode, a constant cantilever deflection is maintained and the force

between the probe and the sample remains constant, thereby creating an image of the surface. It is the quickest and most reliable mode of imaging and it can be used to obtain 3D topographical information on rough surfaces which is what was needed to analyze fabricated microstructures.

II. HYPOTHESIS AND SPECIFIC AIMS

A reasonable amount of research has shown that cell differentiation, proliferation, migration, and morphology are affected by physical factors of the microenvironmental niche. However, few studies have investigated the effects of topography and mechanical factors of the physical microenvironment on stem cell adipogenic differentiation. Therefore, the influence of physical cues in the context of adipogenesis and soft tissue regeneration needs to be elucidated. The working hypothesis of this thesis is that by elucidation of substrate physical effects on cell adipogenic differentiation, one can better understand and control cell differentiation in vitro and ultimately design a more clinically feasible tissue engineered device.

A. Specific Aim 1: Design and fabricate a physical environment that would allow simultaneous observation of mechanical stiffness and surface topography effects on hMSC adipogenic differentiation in terms of lipid production.

Fabrication of substrata will be done using standard lithography techniques. Photolithography is used to generate a patterned surface with parameters in the micron and submicron range. 50 x 50 micron posts with a pitch length of 200 microns. The stiffness of post containing substrates is altered by decreasing the cross linker to base ratio to make posts several folds softer. 10:1 and 30:1 polymer substrates were constructed with the intention of having a one fold difference in stiffness.

B. Specific Aim 2: Examine the effects of topography and topographical stiffness on hMSC adipogenic differentiation.

In order to examine how topography and topographical stiffness affects adipogenic differentiation, cells will be stained with Oil Red O for qualitative and quantitative analysis of lipid formation at three time points of day 4, day 7, and day 14 of differentiation. In addition, relative percent lipid formation will be assessed by image analysis of lipid formation relative to number of cells observed per image.

III. RESEARCH DESIGN AND METHODS

A. Culture and Propagation of Human Mesenchymal Stem Cells

Human bone marrow derived mesenchymal stem cells (hMSCs, 7071R) were obtained from a NIH-funded Gene Therapy Center (Tulane University, New Orleans, LA). Propagation of cells was initiated by thawing and plating in 250 ml (T-75) culture flasks. Cells were cultured under a standard medium of Alpha-Modified Eagle's Medium (α-MEM) with L-glutamine, without ribonucleosides, without deoxyribonucleosides; Gibco, Grand Island, NY supplemented with 15 % FBS, 1% L-Glutamine (2 mM), 1% antibiotics (100 U/mL penicillin and 100 µg/mL streptomycin). Cells were maintained at 37°C in the presence of 5% CO_2/95% air atmosphere. Cell culture media was changed every 2 or 3 days, and cells were passaged at 80 to 90% confluency. Passages between 4 and 10 were used in the experiments. For adipogenic differentiation, cells were incubated in adipogenic induction media (growth medium, 0.5 mM 3-isobutyl-1-methylxanthine (IBMX), 200 µM indomethacine, insulin (10 µg/mL) and 1 µM dexamethasone; Sigma-Aldrich, St. Louis, MO) and medium was changed every other day.

B. Oil Red O Staining for Adipogenic Differentiation

In order to qualitatively and quantitatively measure adipogenic differentiation, Oil Red O, a lysochrome or fat soluble dye predominantly used for demonstrating triglycerides was used. Oil Red O was chosen for its largely deeper red color over Sudan III, also a lysochrome allowing better qualitative and quantification assessment of lipid formation. Firstly, Oil Red O Stock Solution was prepared by mixing 0.35 grams of Oil Red O (Sigma,

Cat # O-0625) with 100 ml of isopropanol. The solution was then allowed to be stirred overnight followed by filtering (0.2 micron) and stored at room temperature. The working solution was then prepared. The solution was then set at room temperature for 20 minutes followed by filtering (0.2 micron). Medium was removed from each sample substrate. Each sample was then washed twice and fresh formalin was added to each sample followed by at least one hour incubation. After fixation, samples were washed with de-ionized water twice followed by washing with 60 percent isopropanol for 5 minutes at room temperature in order to eliminate background staining. After aspiration of 60 percent isopropanol, Oil Red O working solution was added and samples were incubated at room temperature for 10 minutes. Oil Red O solution was then aspirated followed by immediate addition of de-ionized water. Cells were washed four times with de-ionized water. Samples were then incubated in DAPI solution for 5 minutes in order to stain and quantify adipogenic differentiation relative to number of cells per view by staining DNA content of cells.

C. Fabrication of Master Mold

The desired microtextured silicone surfaces were created using standard lithography techniques in the Nanotechnology Core Facility located at the University of Illinois at Chicago. The first step of the fabrication process was to design the pattern of interest using AutoCAD. First the design of interest was drawn out in CAD. The chrome mask to be patterned was 16 in^2 in size. Figure 2 is a schematic summarizing the various steps involved in ultimately fabricating the master utilized to create silicone molds in order to be used in cell culture experiments. The ultimate pattern to be generated was an array of 50 x 50 micron size posts with a 200 micron pitch and a submicron size height. The mask was coated with

positive photoresist. The mask was then developed in a positive photodeveloper and the exposed regions using the Pattern Generator were removed leaving the patterned area designed in AutoCAD, transparent. The final mask was then used to transfer the desired pattern to PDMS substrates of varied stiffness.

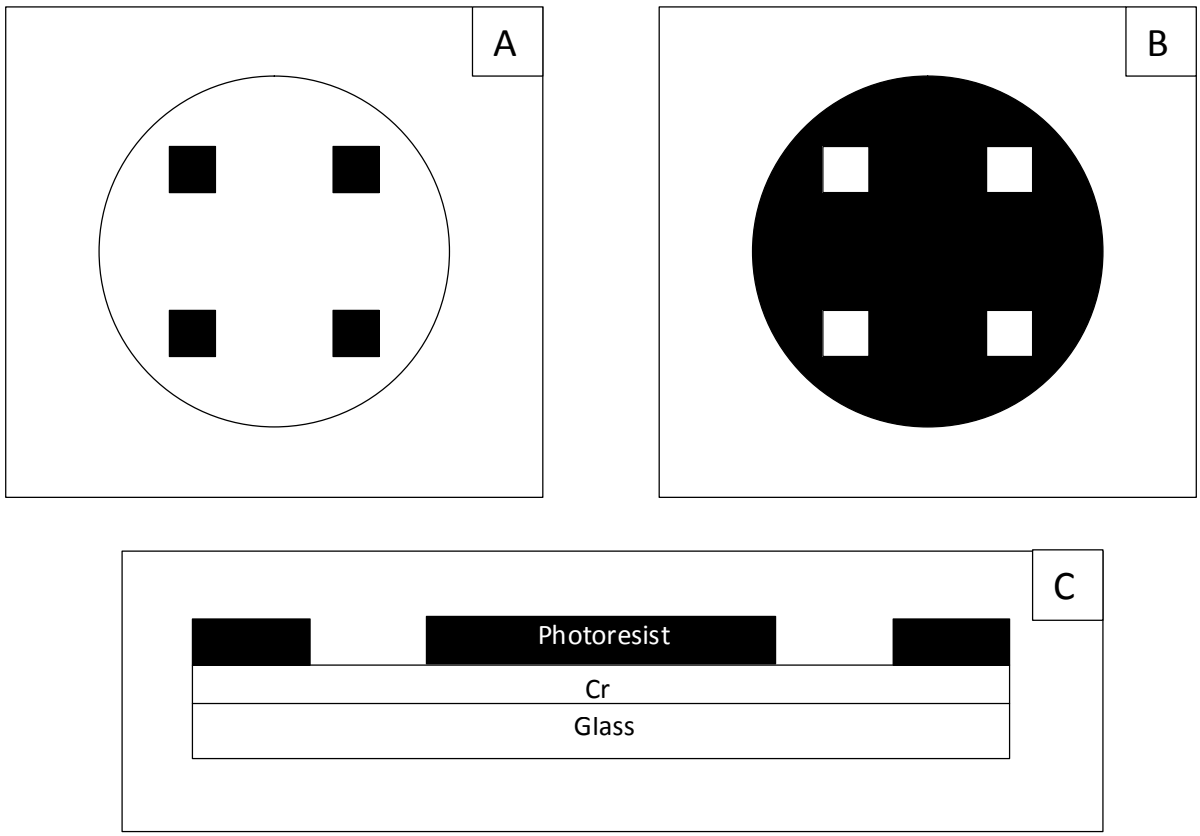

Figure 2. Fabrication of Master Mold A: Sample image of mask design in AutoCAD. B: Mask after pattern generator exposure, development and etching. C: Cross sectional view of mask after pattern fabrication on mask.

D. Preparation of Silicone Substrates for hMSC Culture

In order to create the most suitable cell culture conditions for hMSC seeding, the surface chemistry of silicone substrates required modifications in order to induce proper cell attachment and spreading. There were several options with respect to how the surface chemistry could be altered based on reviewing the literature. One method was to treat silicone substrates with HCL otherwise known as acid treatment. Another method was to coat the surface with an extracellular matrix protein. Lastly, plasma oxidation surface treatment was done as it has shown to facilitate alterations in the surface chemistry of the prepared PDMS substrate surface by temporarily adding silanol groups (SiOH) to the surface or in other words making the surface temporarily hydrophilic (23). Ultimately, optimal cell attachment, survival and proliferation were seen with oxidation of PDMS substrates using the plasma oxidation surface treatment followed by coating with collagen.

In order to prepare sample PDMS substrates for cell culture, not only was the surface treated for optimal cell attachment but samples needed to be sterilized to avoid cell contamination. Briefly, PDMS under the product name of Sylgard 184 (Dow Corning Corporation, Midland, MI) was ordered. The commercially available Sylgard package contains two components, the elastomer base component (SYLGARD 184 Silicone Elastomer Base) and a cross linking or curing agent. The mixture ratios used for this experiment were 10:1 (m/m) and 30:1 (m/m) base to cross linking agent. It was important that the mixing be done in various directions and not just a clockwise direction. If thorough mixing is not achieved, PDMS will not crosslink properly. This will affect curing and ultimately the chemistry of the substrate.

After thorough mixing, the mixed solution was then degassed by being placed in an Isotemp Vacuum Oven Model 280A (Fisher Scientific) attached to a vacuum (Maxima C Plus Vacuum Pump Model M6C, Fisher Scientific) and degassed for about 5-10 minutes. The solution was then poured onto the master which was already sterilized, air dried, and surrounded by aluminum foil in order to prevent outflow of PDMS while it is placed in a heating oven for curing. A schematic summarizing the process of sample preparation for culture is shown in Figure 3.

The mold was then degassed an additional time due to bubbles that were created by pouring the PDMS solution on the master. The solution was then placed in an oven set at a temperature of 75 degrees Celsius for about two hours and thirty minutes. After curing was done, the molds were allowed to cool down to room temperature. A scalpel and tweezers were used to cut and separate the PDMS mold from the chrome master. A hallow punch set (Mayhew Tools) size 9/16 inches was then used to create samples to be placed in each well of a 24 well plate (Fisher Scientific). At this point the samples were ready to be sterilized and surface treated for cell culture.

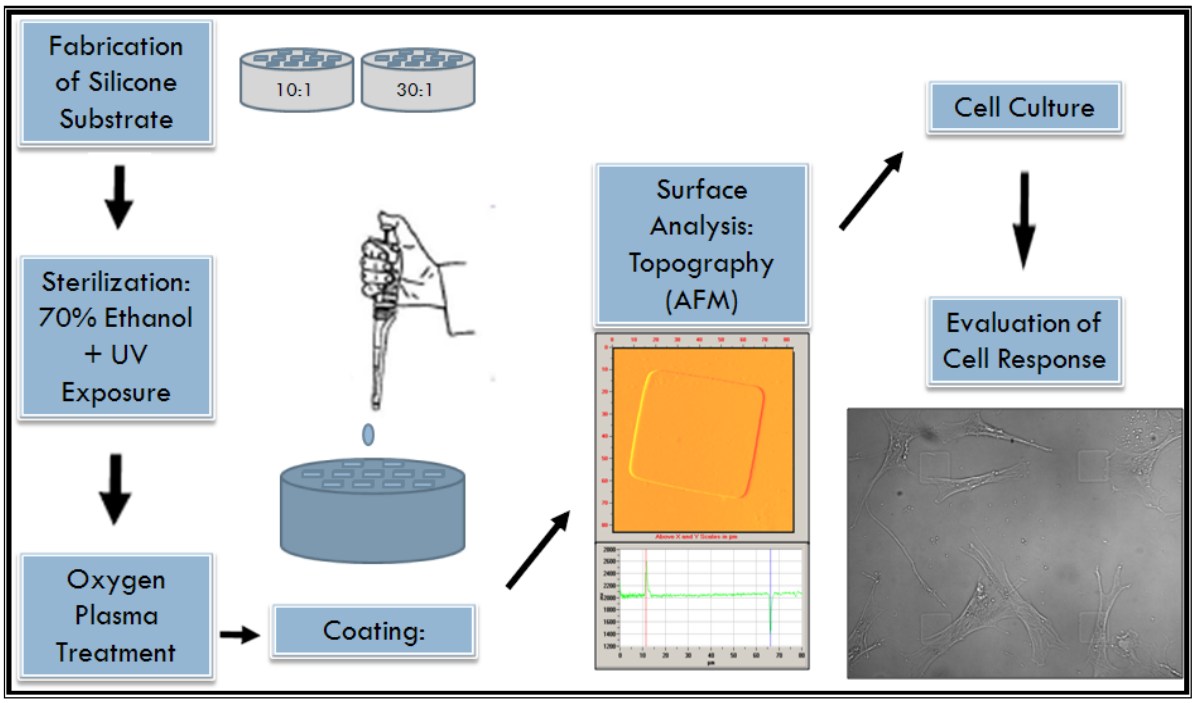

Figure 3. Process of silicone substrate preparation for cell culture and experimental analysis where substrates were sterilized, surface treated in order to promote optimal cell adhesion followed by topographical analysis using AFM and cell seeding for experimental analysis.

E. Stiffness Measurement of Scaffolds by Atomic Force Microscopy

The elasticity of the scaffolds was measured with a Novascan atomic force microscope (Novascan Technologies, Ames, IA) mounted on an inverted Nikon microscope (Tokyo, Japan). A piezoelectric scanner with a maximum XY range of 80 X 80 μm and a vertical z range of 7.3 μm was used. Soft silicone nitride cantilevers (Veeco, Santa Barbara, CA) 100 μm long, were calibrated by the thermal fluctuation method in the air, with a typical spring constant value of 0.12 N/m. Borosilicate glass beads (10 μm in diameter) glued onto the cantilever served as scaffold indenters. The scaffolds were mechanically probed with AFM at several locations over a 15 X 15 μm area. The acquired force curve measured the cantilever deflection and corresponding applied force at every vertical z-position of the cantilever as it approached and indented the scaffold. The cantilever descended towards the scaffold at an approximately 2 μm/s velocity in order to avoid viscous effects of solution and cell until a trigger force of 3 nN was reached. This is to ensure that the force measurements are dominated by the scaffold elastic behavior. The force distance curves were collected and analyzed according to the Hertz model, which relates the loading force, F, with indentation depth δ:

$$F = \frac{4}{3}\frac{E}{(1-\nu^2)}\delta^{3/2}\sqrt{R},$$

where ν is the cellular Poisson's ratio, R is the radius of the spherical indentor (5 μm), E is the local Young's elastic modulus, and δ is the cell indentation depth. The cellular Poisson's ratio was assumed to be 0.5, which treats the cell as an incompressible material. The bidomain polynomial model (linear for pre-contact and Hertz's equation for post-contact, with adjustable contact point z_o) was fit to the experimental force curve using a standard

least-squares minimization algorithm. The fit yielded two unknown parameters: the contact point of AFM probe with the cell at z_o and pointwise apparent elastic modulus E. Distributions for the measured E values were plotted, and the average Young's modulus for each cell type and experimental condition was calculated and subjected to t-test at an α level of 0.05 (26).

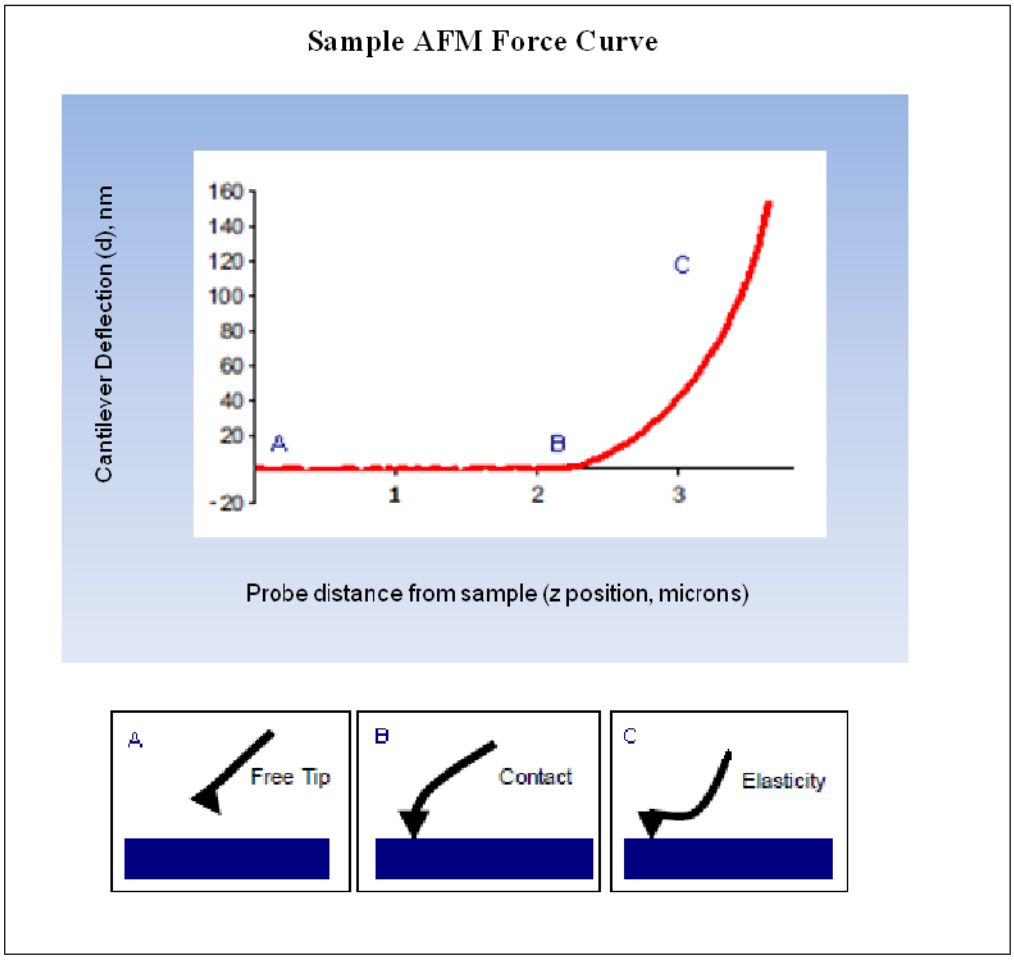

Figure 4. Sample force curve showing various probe and sample interactions. Indentation obtained and used in calculation of elasticity can also be observed. Figure adapted from Titushkin et al., 2011.

F. Characterization of PDMS Topology Using AFM

The characterization of PDMS topography was done with a Novascan atomic force microscope (Novascan Technologies, Ames, IA) mounted on an inverted Nikon microscope (Tokyo, Japan). A piezoelectric scanner with a maximum XY range (Scan size) of 80 X 80 μm and a vertical z range of 7.3 μm was used. First, the laser beam was directed onto the back of the cantilever. This was done by using the X and Y laser position controls to adjust the path of the laser. The next step was to adjust the optical detector position. For contact mode imaging, this was done by positioning the beam at the intersection of the vertical green line and the innermost target circle of the beam align window available in the main toolbar of the Novascan software which serves to graphically represent where the laser beam is striking the optical detector. Scan size was defined to be the length of one side of the square area scanned. Hence, a value of 80 microns means an area of 80 microns x 80 microns was scanned. Other scan parameters such as scan direction, X center, and Y center were assigned so as to set parameters for the probe to follow as it rasters over the area of interest, in this case a single silicone post. The center was assigned relative to surface area of the pattern of interest. After parameters were set, the probe was engaged with the surface and the scan was raster scanning was accomplished. Following the scan, images were analyzed. X, Y, and Z dimensions of the image were analyzed in order to obtain exact dimensions of each post. In addition, images were taken from the fabricated mask using a Nikon microscope in order to obtain additional data relative to the pitch length of posts which was designed to be 250 microns in AutoCAD. These images along with AFM images can be observed in the results section.

G. Analysis for Adipogenic Differentiation

Image analysis was done in order to determine relative percent lipid formation as a result of introduction to a single physical cue or multiple physical cues. This was done by acquiring four images per sample for each condition. Specifically, each fixed sample was washed and stained for visualization of lipid and nuclei. There were three images taken per view all at a 20x magnification. A DIC image was first taken in order to see the cell relative to the location of topography. This was followed by acquiring an image of lipid content and nuclei. Nuclei staining was done in order to determine relative percent lipid area formation per image taken for analysis. Specifically, a cell count was done followed by quantification of percent lipid area stained. This was done for four views per sample and the relative lipid formation was quantified by dividing the obtained percent lipid formation quantity by number of nuclei. A brief schematic of this process is shown below in Figure 5.

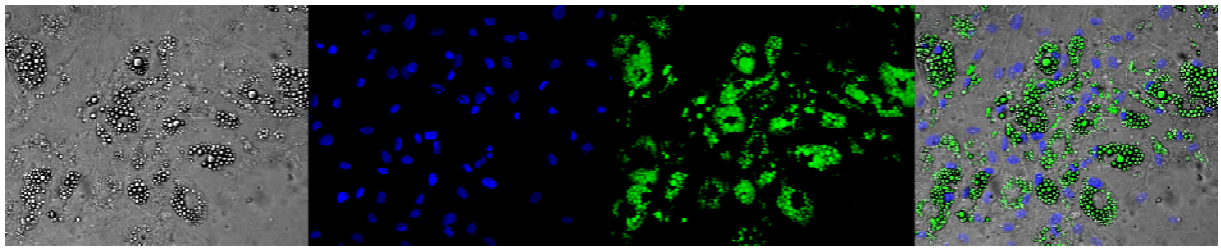

Figure 5. Lipid area quantification analysis. Summary of the image processing and analysis done to determine relative lipid content per sample.

H. F-Actin Staining

15 µg TRITC-conjugated Phalloidin (Chemicon) was resuspended in 250 µL of methanol and diluted 500x for actin cytoskeleton labeling. Samples for each condition and each trial were imaged for F-actin after seeding. The samples were first fixed with 10 percent formalin for 10 to 15 minutes followed by permeabilization with ice cold (-20°Celsius) acetone for 3 minutes. After washing samples twice with buffer solution, the samples were incubated with TRITC-conjugated Phalloidin. After washing an additional two times, the cells were incubated in DAPI solution for 5 minutes at room temperature in order to obtain images of cell nuclei.

I. Sample Imaging

After staining, the images were recorded using a Nikon microscope (Eclipse E-800, Nikon, Melville, NY) in differential interference contrast, bright-field, and epifluorescence modes. This was done with an X-Cite 120 mercury lamp fluorescent illumination system, a CCD camera (CoolSnap fx; Roper Scientific, Tucson, AZ), and a 60X Plan Apo objective (NA 1.4) objective. Images were processed using a MetaMorph image processor (Universal Imaging, West Chester, PA). Cells grown on PDMS scaffolds were handled and removed from the wells using tweezers in order to image the cells on top of the scaffolds. To accomplish this, a small spatula was used to carefully prod the periphery of the scaffold, to remove its attachment to the well. It was also used to gently nudge the scaffold to remove its adhesion from the bottom of the well, taking care not to scrape the top surface of the scaffold where the cells reside. The scaffold was then transferred and placed on a glass slide, cell side up whereupon the cells could be imaged.

IV. RESULTS

A. Analysis of Fabricated Micro-topographical Features Following Wet Etching

After fabrication of patterned mask using photolithography techniques, patterns were observed and measured under a microscope in order to ensure the existence of correct pattern dimensions. Distance of the aligned lines in both the X and Y direction in addition to magnification are summarized on the top corner of each image showing pattern features to have a 50 x 50 micron size and a pitch length of about 200 microns (Figure 6).

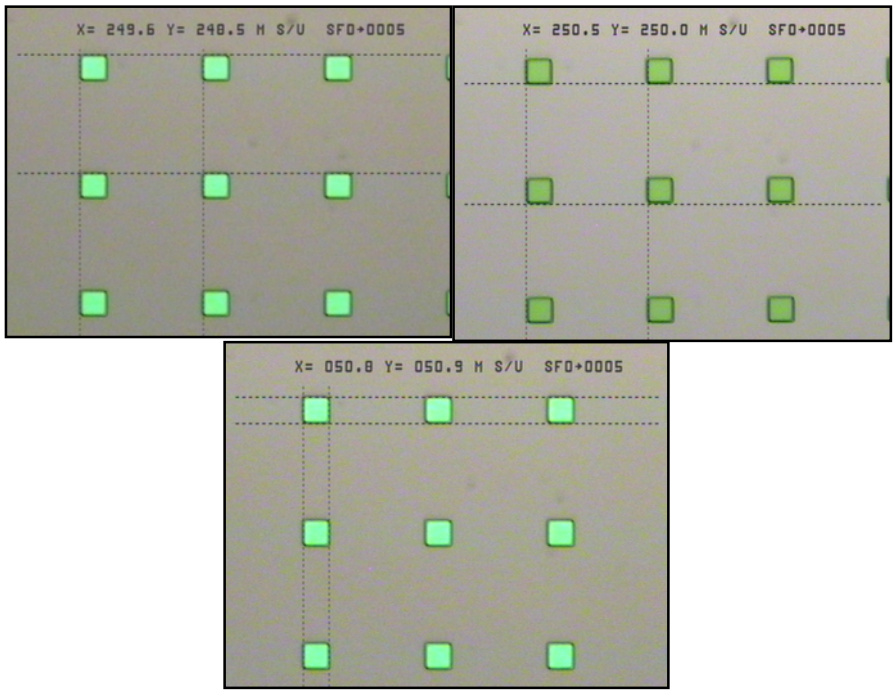

Figure 6: Master mold pattern size analysis of feature parameters in addition to pitch size following wet etching. Summary on top of images show features to be approximately 50 microns x 50 microns and to have a 200 micron pitch length.

B. AFM Analysis of Topographical Structures

1. Measurement of feature length along the X and Y axis.

After transferring the micro patterns to silicone substrates, the samples were rinsed in ethanol and UV treated for sterilization. Samples were then plasma treated and coated with collagen at a concentration of 20 ug/cm^2. Then samples were imaged using atomic force microscopy in contact mode. The imaging was done after all treatment processes to ensure micro pattern dimensions to which cells be exposed to are measured. The measurement made based on Figure 8 below was 54. 797. In addition the same measurement made in the Y direction gave a measurement of 50.597 microns.

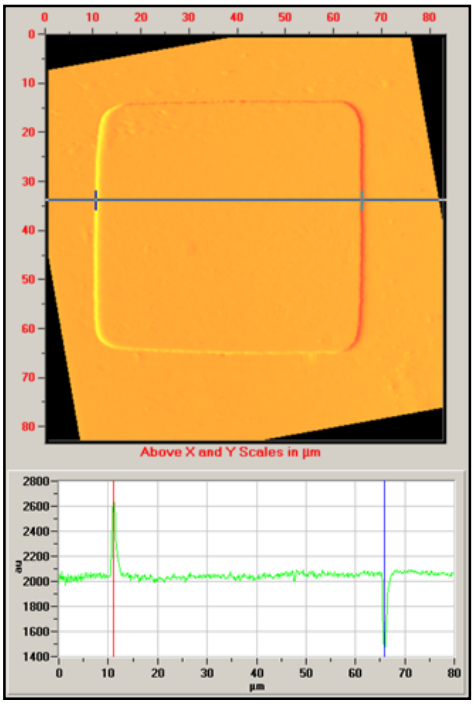

Figure 7. Contact mode imaging of micro-topography and analysis of X axis dimension using Novascan software by measuring the distance between deflection peaks of post.

2. Measurement of feature height.

When performing contact mode imaging using an atomic force microscope you obtain several images or sets of data. Two of these sets of data are called Z-Height and Deflection. The image below gives a cross-sectional view of a single post. Ultimately, the height measured for the post was 114 nm (Figure 8).

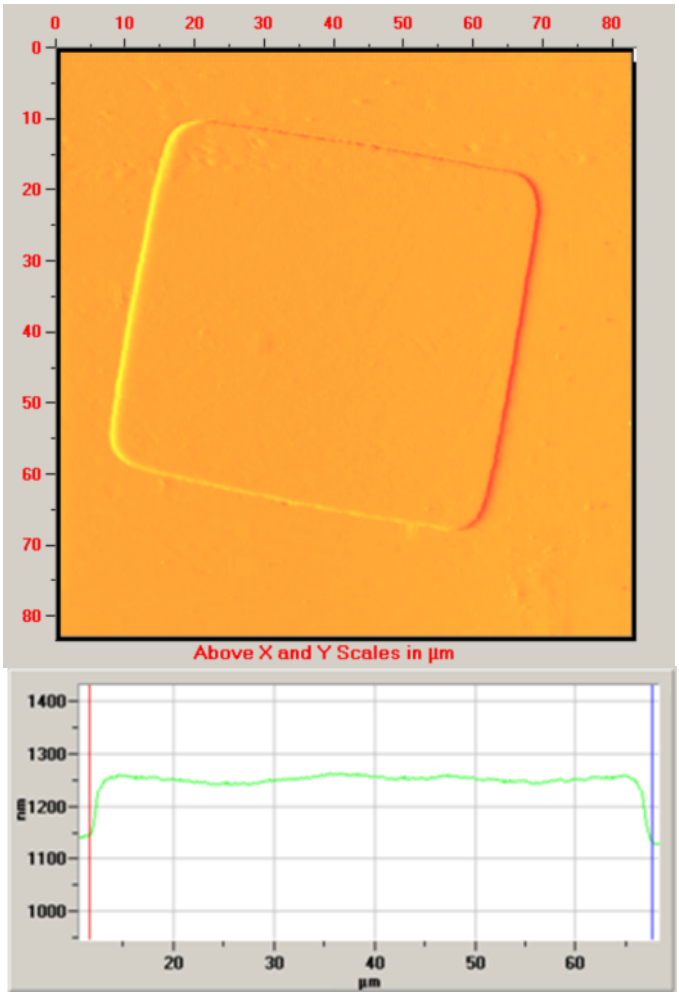

Figure 8. Image of surface plot showing cross-sectional view of topographical feature. The surface plot shows an approximate feature height of 114 nm.

C. Concentration of Cross-linker to Base Determines Micro-topography stiffness

AFM measurements were performed in order to determine the elastic modulus or stiffness of PDMS scaffolds of two different concentrations. A scaffold made with a polymer base to cross-linker ratio of 10:1 was found to have a stiffness of 2.76 MPa while a 30:1 mix was found to have a stiffness of 0.26 MPa. These concentrations were chosen in order to have an order of magnitude difference in stiffness of scaffolds. This would allow us to possibly see a different effect on cell behavior.

D. Oil Red O Staining of hMSCs On 10:1 Patterned and Plain 10:1 Substrates

Oil red O staining for lipid droplet formation done on days 4, 7, and 14 can be observed in Figure 9 for hMSCs grown and differentiated on substrates with and without posts. Lipid droplets reminiscent of adipogenic differentiation are stained red. Cells appear to be differentiating in colonies more on patterned substrates relative to plain substrata. Lipid droplet formation on plain 10:1 substrata appear to be more evenly distributed at days 4 and 7 compared to patterned substrates. Positive staining was seen as early as day 4 of differentiation. Differentiation also appears to be more on patterned substrates (Figure 9).

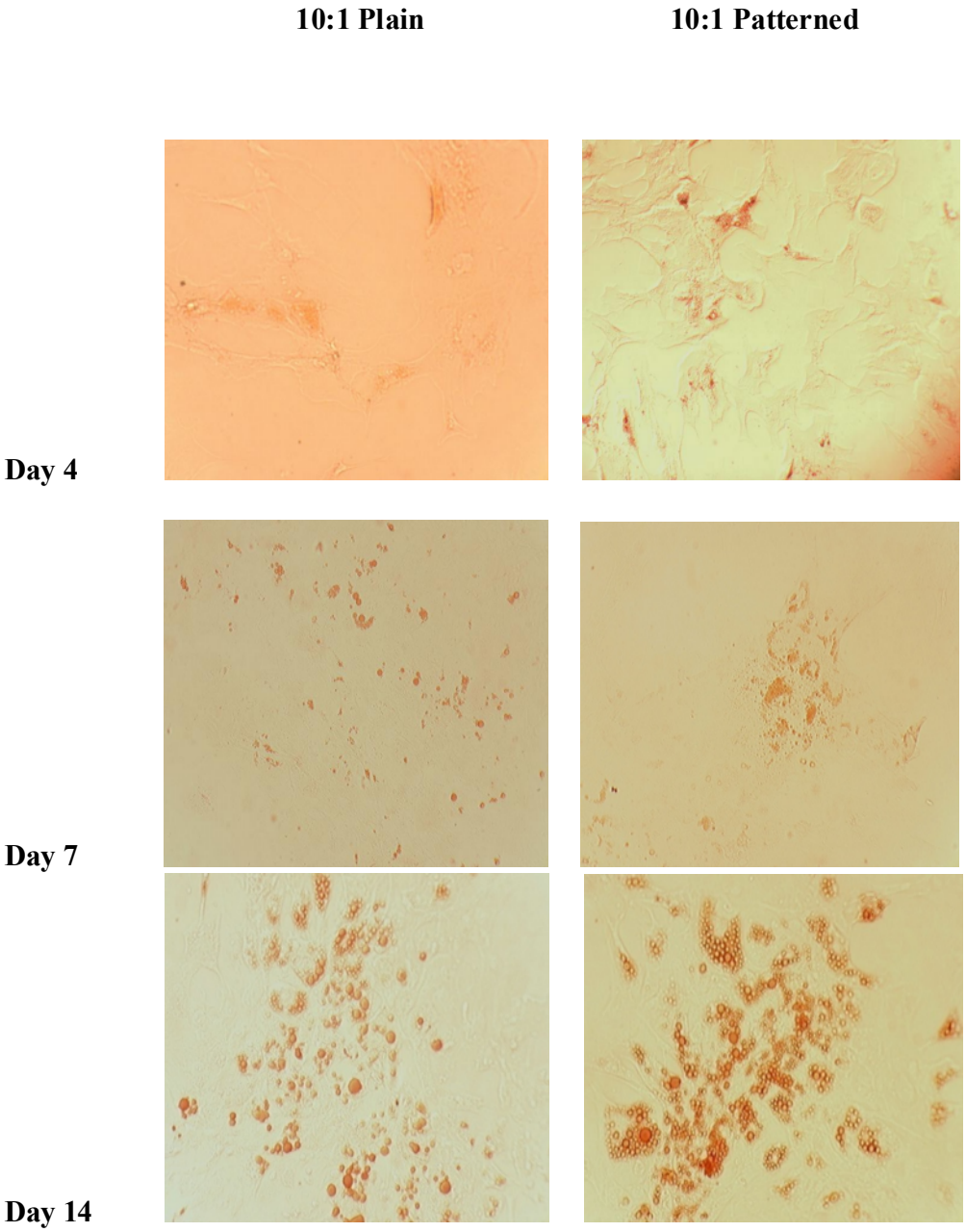

Figure 9. Day 4, 7, and 14 of Oil Red O stained lipid droplets formed showing adipogenic differentiation of hMSCs. Cells on patterned 10:1 substrates seem to be growing more in aggregates compared to plain substrates.

E. Oil Red O Staining of hMSCs On 30:1 Patterned and Plain 30:1 Substrates

Oil red O staining for lipid droplet formation done on days 4, 7, and 14 can be observed in Figure 10 below for hMSCs grown and differentiated on 30:1 substrates with and without posts. Lipid droplets reminiscent of adipogenic differentiation are stained red. Similar to 10:1 (stiffer) substrates, cells appear to be differentiating in colonies more on patterned substrates relative to plain substrata. Lipid droplet formation on plain 10:1 substrata appear to be more evenly distributed at days 4 and 7 compared to patterned substrates. Unlike 10:1 substrates, lipid droplets appear to be more evenly distributed even at day 14 of differentiation. Positive staining was seen as early as day 4 of differentiation. Lipid droplet formation also appears to be more on patterned substrates (Figure 10).

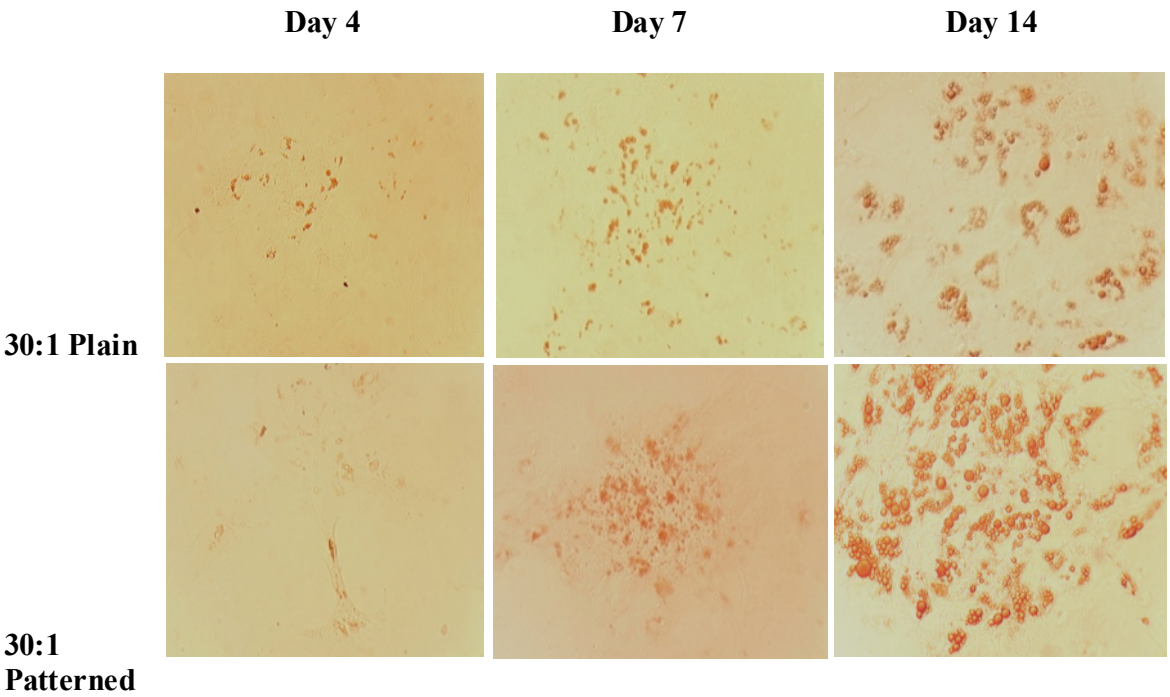

Figure 10. Oil Red O lipid staining of differentiated hMSCs at days 4, 7, and 14 on patterned and un-patterned PDMS substrates with varied post stiffness. Images are taken at 20x magnification.

F. DIC Images of Aggregate Formation on Patterned Substrates Showing Location of Colonies Relative to Posts

Images in Figure 11 display how cells formed colonies on patterned substrates. Lipid formation seems to be more around the location of posts. Increased initial cell-to-cell contact and colony formation is likely to have increased initial differentiation speed of cells seeded on patterned substrates. The distanced posts in this particular patterned substrate seems to have encouraged colony formation around single posts. Similarly, this can be observed at a higher magnification in Figure 12.

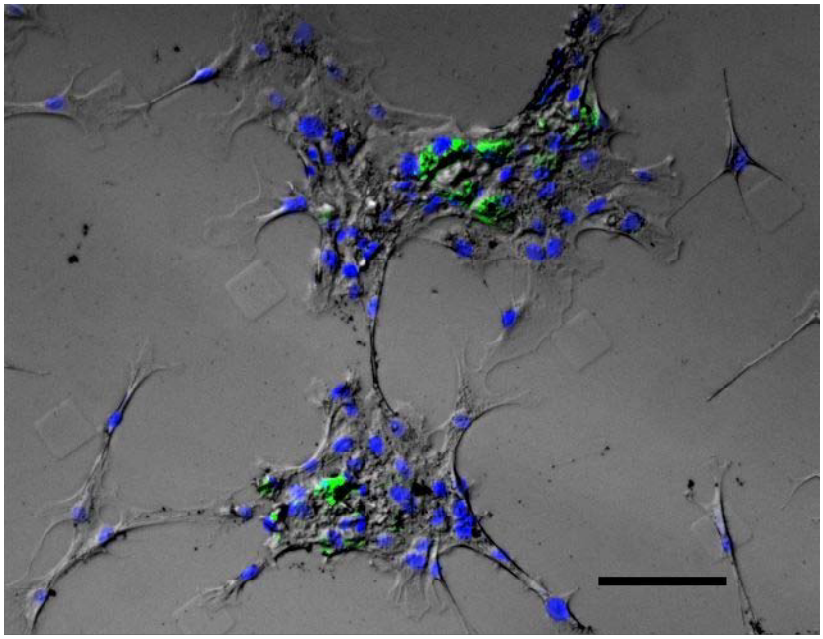

Figure 11. 10x image showing single cell colony formation on posts with lipid formation mostly around the location of the posts. (Scale bar represents 100 microns)

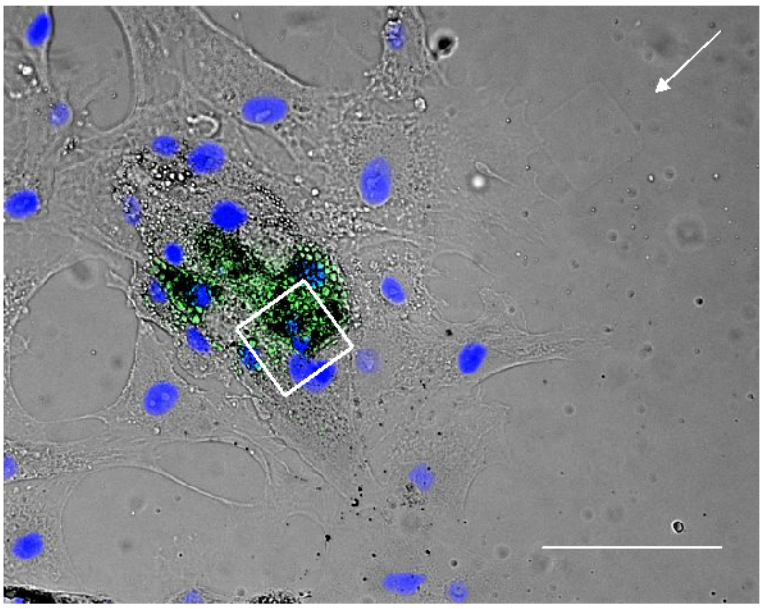

Figure 12. 20x image of cell aggregate on top of post. Again, lipid formation is mostly around post area. Arrow indicates location of a post. Scale bar represents 100 microns.

G. Actin Cytoskeleton Staining of hMSCs On Posts With Varied Stiffness

Actin cytoskeleton of hMSCs were visualized 24 hours after seeding. Actin cytoskeleton of cells on stiffer (10:1) posts displayed a more pronounced actin cytoskeleton structure with more stress fibers near the portion of the cell located on the post where as cells on softer (30:1) posts displayed a less pronounced actin cytoskeleton structure with the majority of filaments in close proximity of the post (Figure 13).

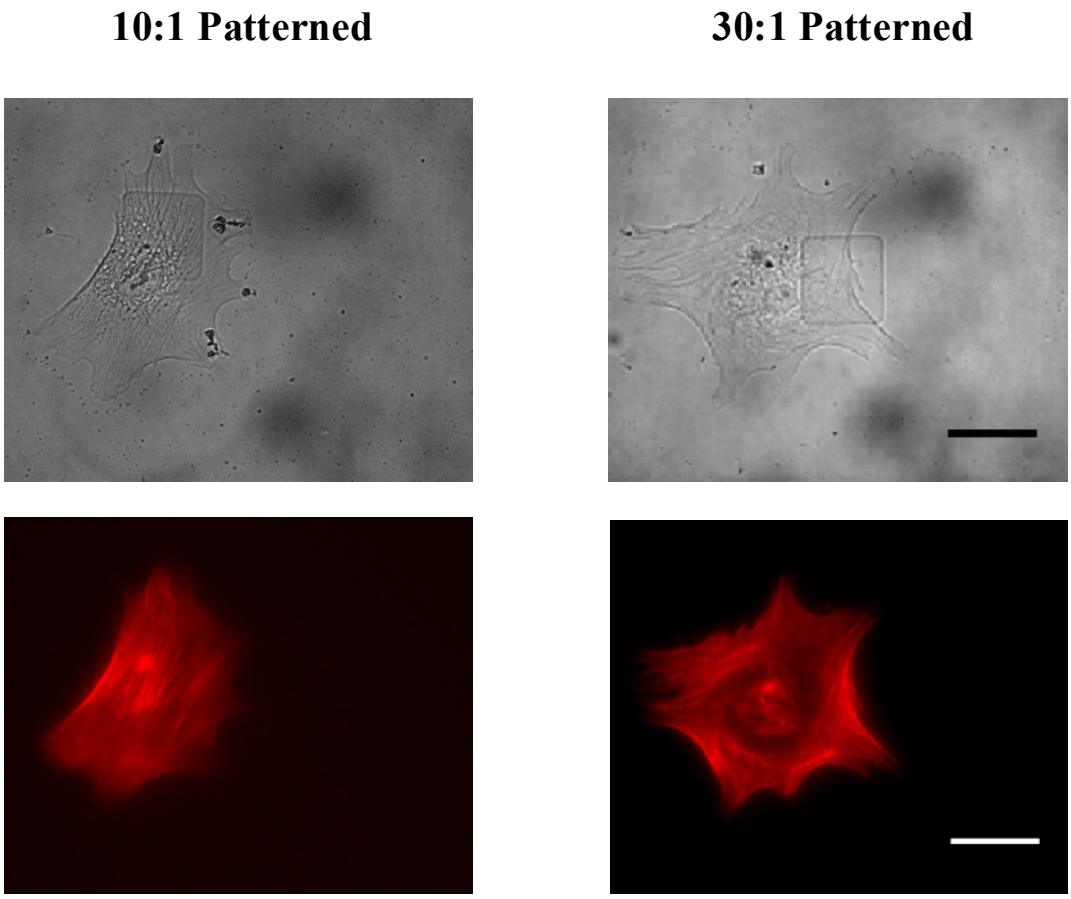

Figure 13. 60x images of undifferentiated hMSCs seeded on 10:1 and 30:1 PDMS substrates and visualized 24 hours post seeding. Top row images demonstrate DIC images of cells on post. Bottom row images show identical cell stained for actin (TRITC-conjugated Phalloidin, pseudocolored red). (Scale bar represents 50 microns)

H. Relative Percent Lipid Area Formation

1. hMSCs Cultured On 10:1 Plain vs. Patterned Substrates

Stained samples for lipid formation were imaged at 20x magnification. After percent area calculation and dividing by the number of cells counted in the same image, it was determined that at days 4 and 7, there was significantly higher lipid formation on patterned substrata. However, at day 14, there was no significant difference observed when comparing plain and patterned 10:1 substrates (Figure 14).

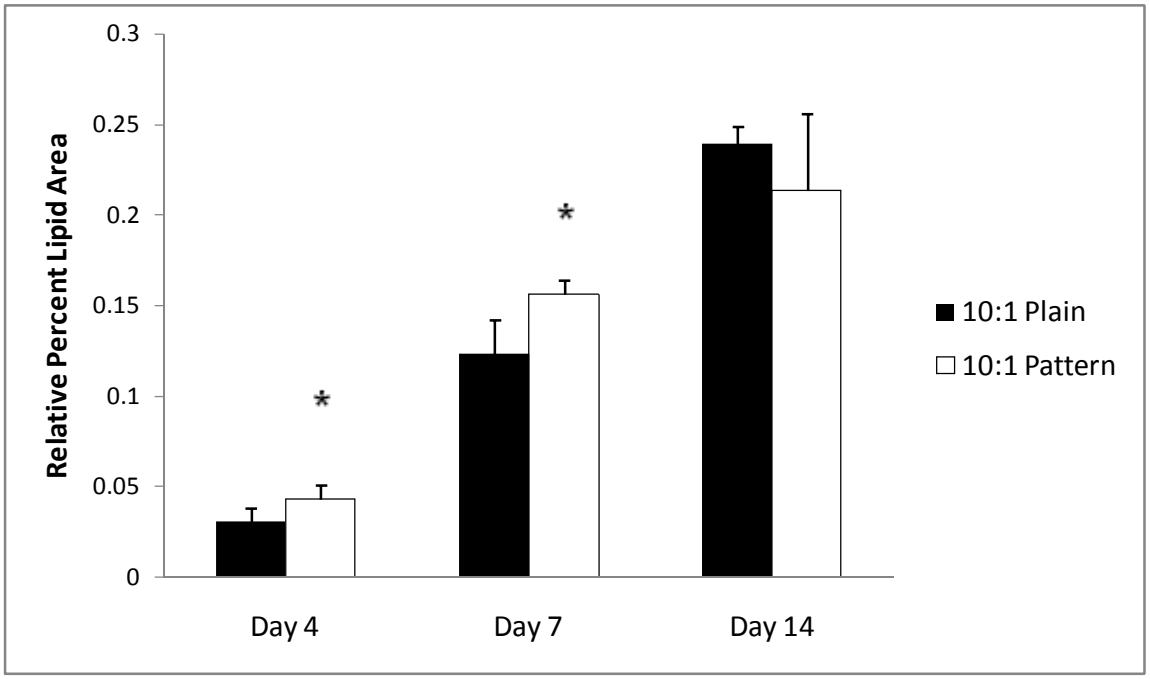

Figure 14. Relative percent lipid area comparison between cells differentiated on 10:1 plain vs. 10:1 patterned substrates. (Significant difference: $p<0.05$)

2. hMSCs Cultured On 30:1 Plain vs. Patterned Substrates

Stained samples for lipid formation were imaged at 20x magnification. After percent area calculation and dividing by the number of cells counted in the same image, it was determined that at days 4 and 7, there was significantly higher lipid formation on patterned substrates. However, at day 14, there was no significant difference observed when comparing plain and patterned 30:1 substrates (Figure 15).

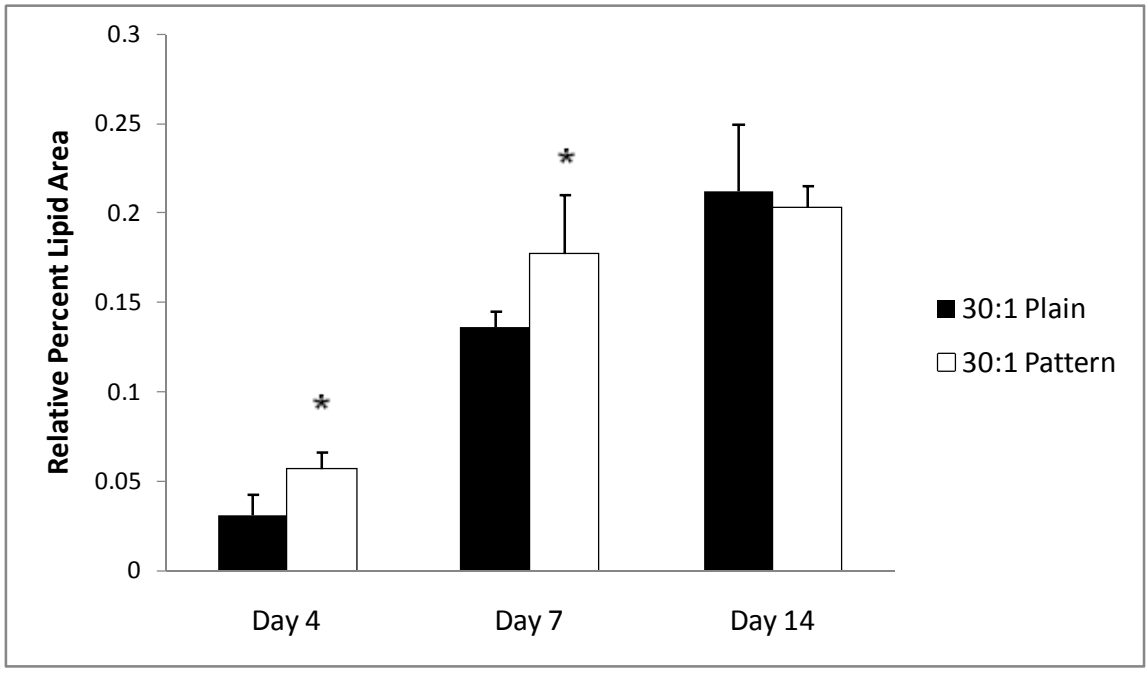

Figure 15. Relative percent lipid area comparison between cells differentiated on 30:1 plain vs. 30:1 patterned substrates. (Significant difference: $p<0.05$)

3. hMSCs Cultured On 10:1 Plain vs. 30:1 Plain Substrates

It was determined that at days 4, 7 and 14, there was no significant difference in relative percent are formation when comparing 10:1 vs. 30:1 plain substrates. There was less percent lipid area observed at day 14 of differentiation on 30:1 plain substrates (Figure 16).

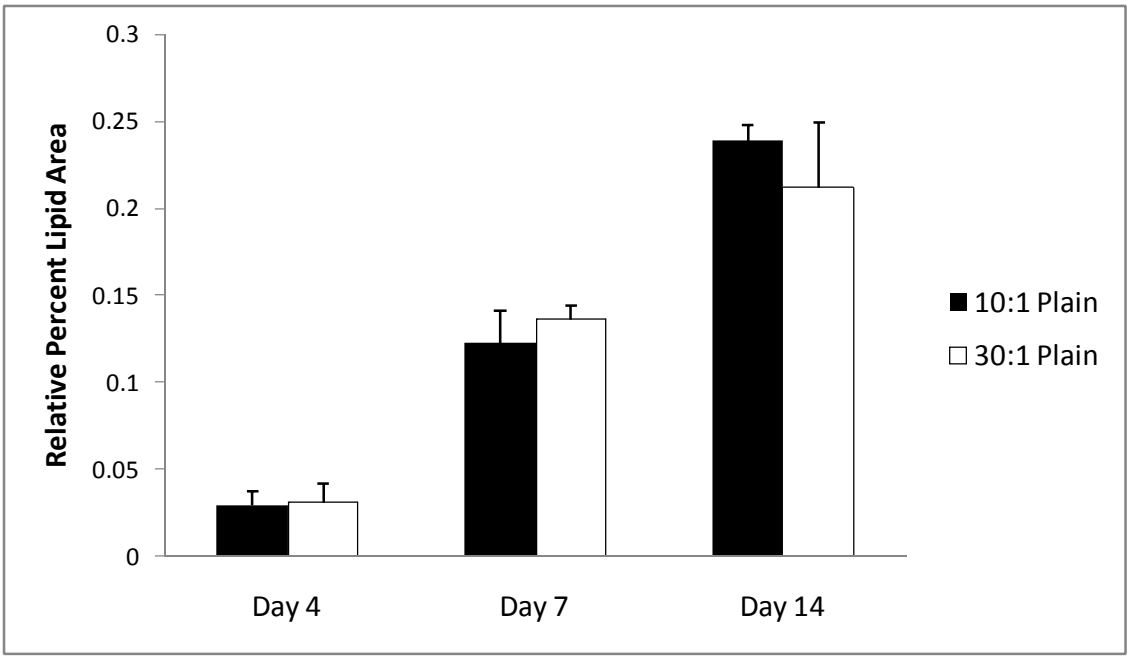

Figure 16. Relative percent lipid area comparison between cells differentiated on 10:1 plain vs. 30:1 plain substrates. No significant difference was observed at all three time points.

4. hMSCs Cultured On 10:1 Patterned vs. 30:1 Patterned Substrates

When comparing lipid area covered by 10: 1 Patterned and 30:1 Patterned substrates, there was no significant difference found at days 7 and 14 of differentiation. Interestingly, there was a significantly higher percent lipid area found at day 4 of cells on 30:1 patterned substrates. There was less percent lipid area observed at day 14 of differentiation on 30:1 patterned substrates (Figure 17).

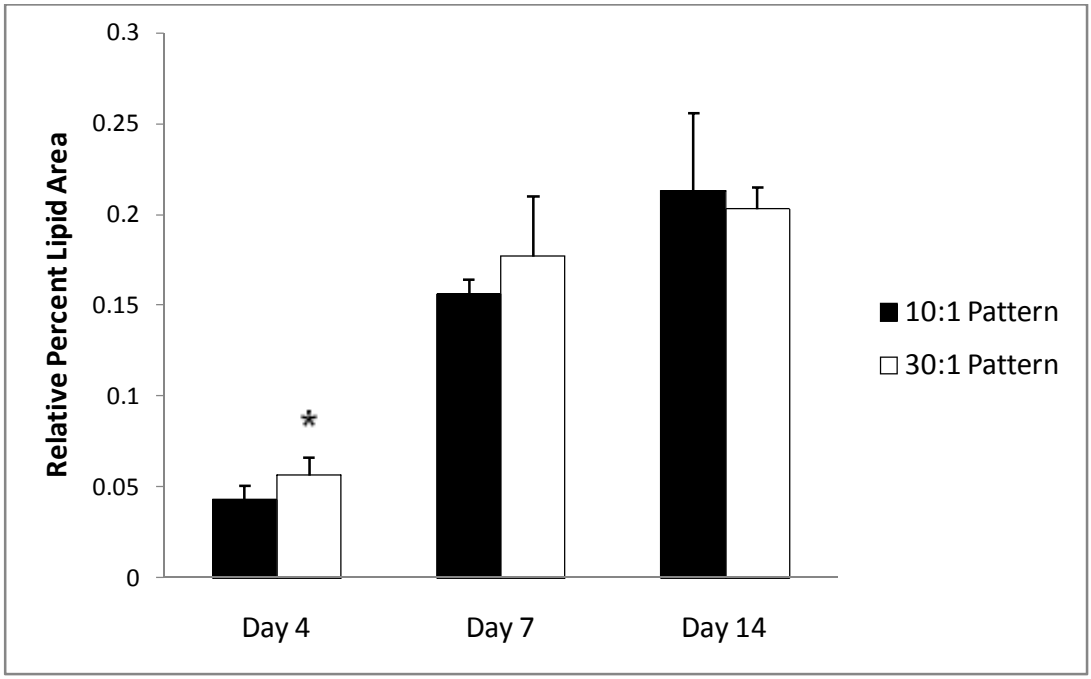

Figure 17. Relative percent lipid area comparison between cells differentiated on 10:1 patterned vs. 30:1 patterned substrates. No significant difference was observed on days 7 and 14. 30:1 substrates showed significantly higher percent lipid area. ($p<0.05$)

I. 510 nm Wavelength Optical Density Measurements for Oil Red O Quantification

1. hMSCs Cultured On 10:1 Plain vs. Patterned Substrates

When comparing optical density of 10:1 patterned and 10:1 plain substrates, there was no significant difference found at day 14 of differentiation. Interestingly, there was a significantly higher absorbance found at days 4 and 7 of cells on 10:1 patterned substrates. There was less absorbance observed at day 14 of differentiation on 10:1 patterned substrates (Figure 18).

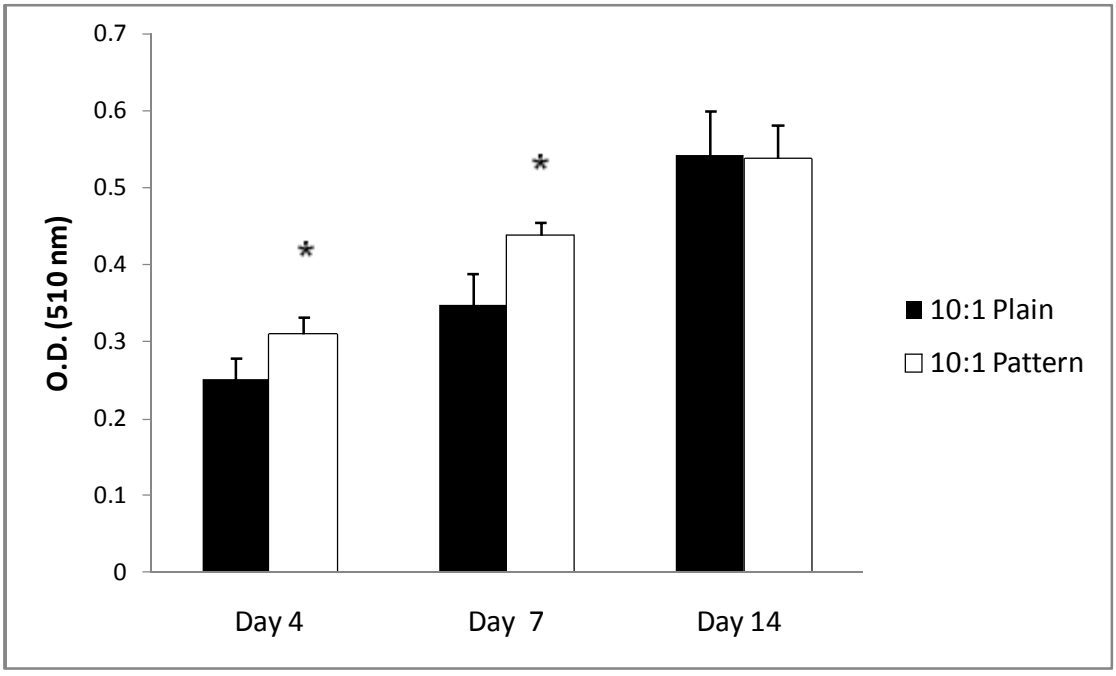

Figure 18. Optical Density of Oil Red O staining comparison between cells differentiated on 10:1 plain vs. 10:1 patterned substrates. (Significant difference: $p<0.05$)

2. hMSCs Cultured On 30:1 Plain vs. Patterned Substrates

When comparing optical density of 30:1 patterned and 30:1 plain substrates, there was no significant difference in absorbance found at days 7 and 14 of differentiation. There was a significantly higher absorbance found only on day 4 of differentiation on patterned substrates (Figure 19).

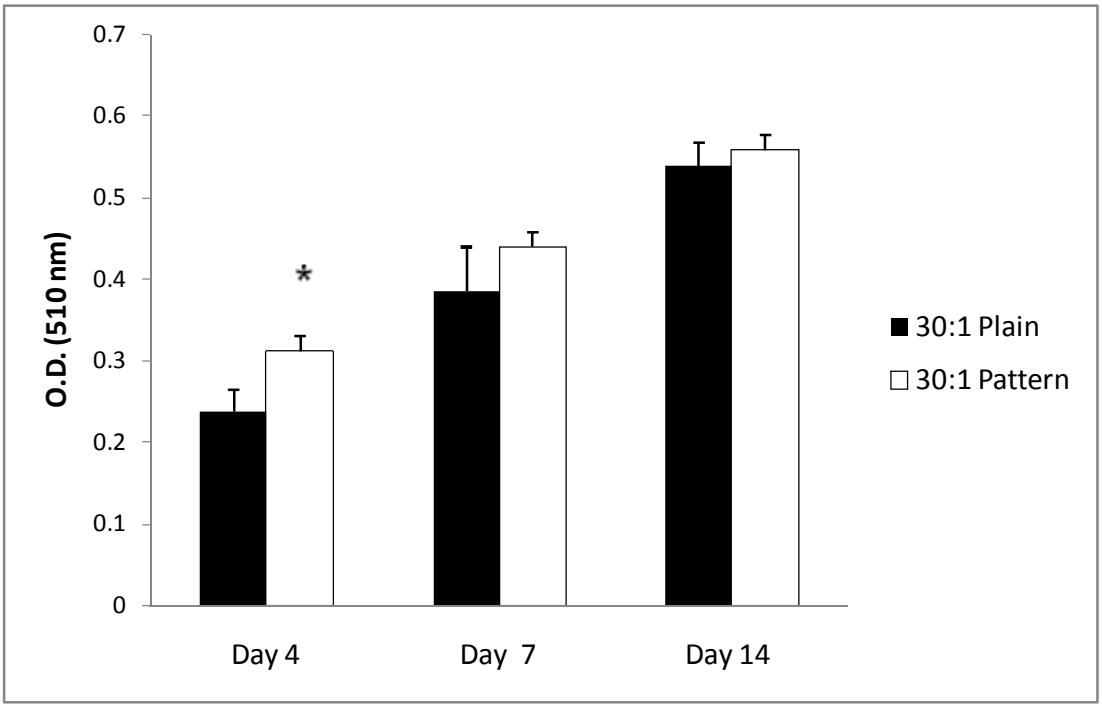

Figure 19. Optical Density of Oil Red O staining comparison between cells differentiated on 30:1 plain vs. 30:1 patterned substrates. (Significant difference: $p<0.05$)

3. hMSCs Cultured On 10:1 Plain vs. 30:1 Plain Substrates

When comparing optical density of 10:1 plain and 30:1 plain substrates, there was no significant difference in absorbance found at days 4, 7 and 14 of differentiation (Figure 20).

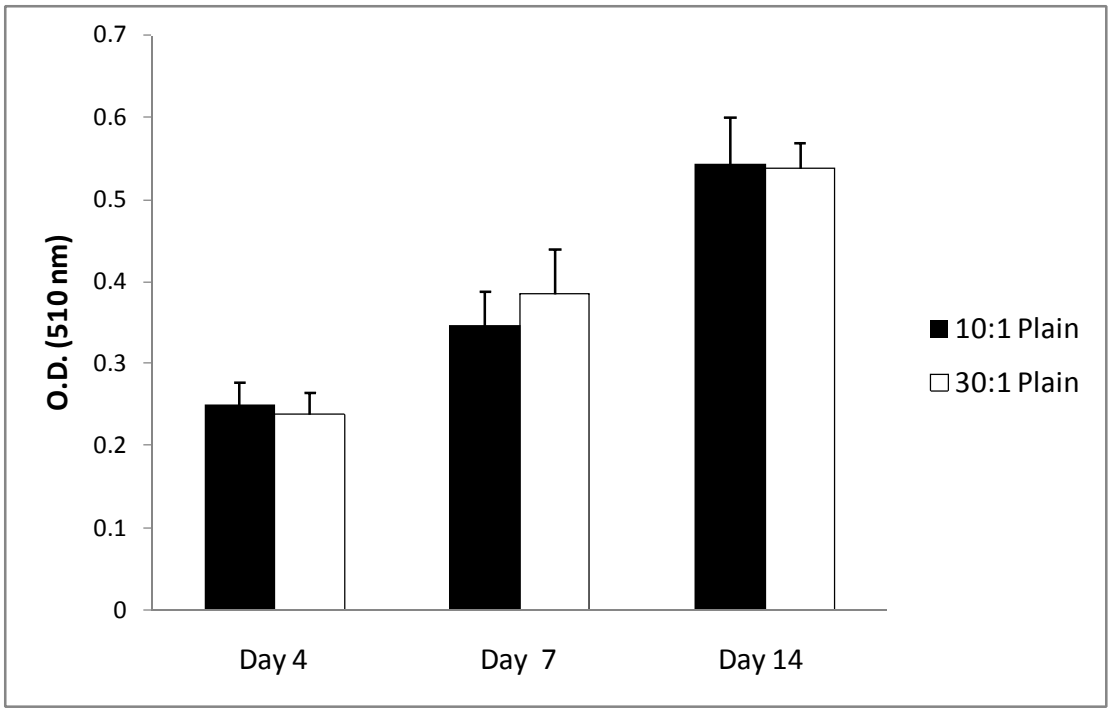

Figure 20. Optical Density of Oil Red O staining comparison between cells differentiated on 10:1 plain vs. 30:1 plain substrates. No significant difference was observed at any of the time points.

4. hMSCs Cultured On 10:1 Patterned vs. 30:1 Patterned Substrates

When comparing optical density of 10:1 plain and 30:1 plain substrates, there was no significant difference in absorbance found at days 4, 7 and 14 of differentiation (Figure 21). However, there was more differentiation observed at day 14 of differentiation.

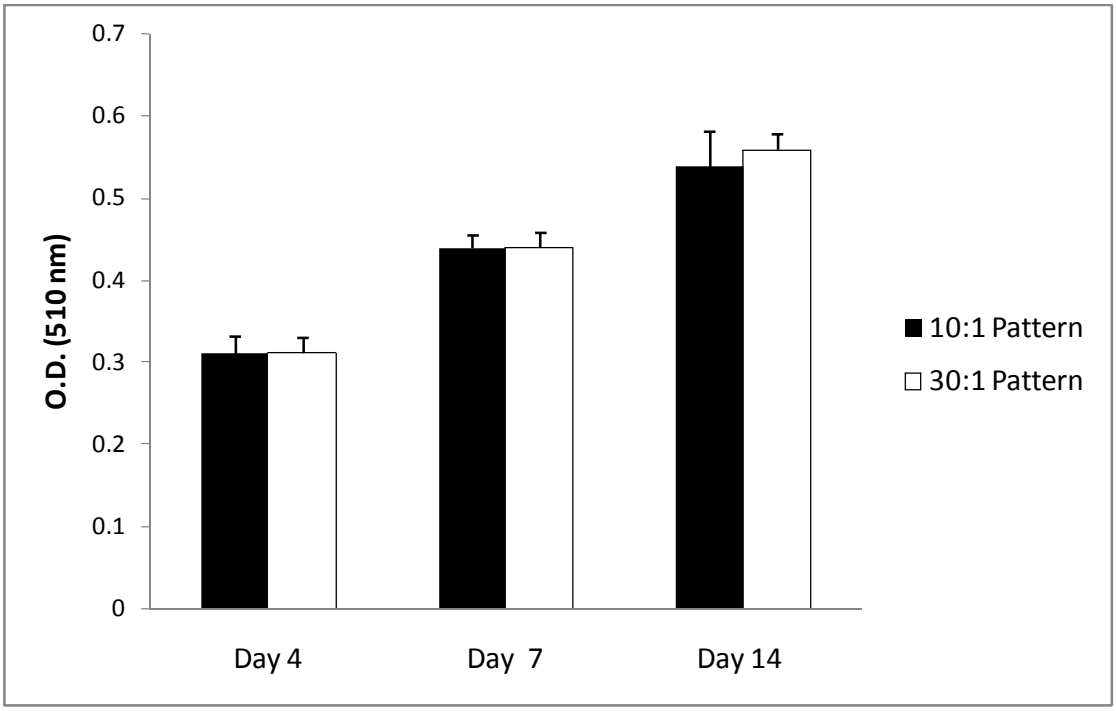

Figure 21. Optical Density of Oil Red O staining comparison between cells differentiated on 10:1 patterned vs. 30:1 patterned substrates. No significant difference was observed at any of the time points.

V. DISCUSSION

One of the aims of this study was to successfully design and fabricate a substrate that would allow simultaneous observation of mechanical stiffness and topography effects on hMSC behavior. Another aim was to examine the effects of topography and topographical stiffness on hMSC adipogenic differentiation by evaluating lipid production using both qualitative methods and quantitative analysis. Oil Red O staining was done for qualitative and quantitative assessment of lipid production at three different time points. Quantitative analysis was done by determining relative percent lipid area formed in addition to observing optical absorbance for quantification of Oil Red O staining. Relative lipid area formation on micro-patterned substrates showed significantly higher percent lipid area at early time points (Day 4, and Day 7) for both 10:1 and 30:1 silicone substrates. At day 14, there was no significant difference observed in relative lipid area.

The significantly higher lipid area observed on days 4 and 7 can be due to cell aggregate formation as a result of the existence of distanced micro-topography. As can be seen in Figure 12, the initial colony formation at an early time point may increase initial cell to cell contact thereby increasing the rate of initial differentiation of hMSCs. In the case of plain substrates, evenly distributed cells induced lipid formation, however, as can be observed in Figures 9 and 10, the lipid droplet formation is less and more evenly distributed on the surface. This may possibly be the reason why no significant difference is seen on day 14 of differentiation. Cell proliferation by then has reached a state where differentiation rates for patterned and plain substrates peak.

In the case where 10:1 and 30:1 plain substrates were compared for amount of relative lipid area, there was no significant difference. Qualitative assessment of hMSCs revealed lipid droplet formation to have similar distribution and quantity when comparing plain substrates with varied stiffness. However, when evaluating adipogenic differentiation with varied topographical stiffness, there was a significantly higher percent lipid area observed on day 4 when comparing relative lipid area formation. The absence of any sort of enhanced differentiation as a result of cell differentiation on softer silicone plain substrates and decreased differentiation at day 14 may suggest that the difference may be due to the difference in polymer surface chemistry as a result of decreased cross-linking and not the stiffness of the substrate itself. Although the stiffness of the 30:1 silicone substrate is one fold less than the 10:1 polymer substrate, the stiffness is still higher than that of natural soft tissue. This may be an explanation for why we could not see synergistic differentiation or a significant difference between plain soft and stiff substrates at all time points. It has been reported that patterned PLLA films via solvent-citing procedures display significantly higher lipid formation on day 10 of differentiation of D1 cells compared to cells grown on plain PLLA substrates (10). However, the effects of the pattern stiffness were not examined in that report. This may suggest that micro-topography can be used as a tool to control the rate of adipogenic differentiation of different types of cells cultured in various types of scaffold materials. Hydrogels such as PEG may be promising polymers for designing future soft tissue engineering models or they have a significantly lower elastic modulus (27).

Although no significant difference was observed when comparing relative lipid area formed for plain substrates with varied stiffness, a significantly higher percent lipid area was observed on day 4 when comparing 10:1 patterned and 30:1 patterned substrates. This

suggests that the micro-topography may play an important role in the initial colony formation which in turn initiates cell to cell contact, thereby accelerating the initial rate of differentiation. Although there was not a significant difference found when comparing plain substrates with varied stiffness, relative percent lipid area formed was for the most part higher on softer substrates. Optical density measurements of cells stained for lipid content was also done in this study in order to quantitatively address lipid droplet formation. The results coincided with the relative lipid area formation data. There was a significant difference in absorbance at early time points of differentiation when comparing patterned to plain substrates. No significant difference was observed when comparing plain substrates with varied stiffness.

In order to observe a possible mechanism for the existence of such differences in differentiation, actin structure of cells was observed. Figure 14 shows actin cytoskeleton organization of hMSCs seeded on patterned substrates with varied stiffness. A less pronounced actin filament structure was observed on soft PDMS substrates where as on stiffer substrates, the actin cytoskeleton structure displayed more pronounced actin filaments. Furthermore, more stress fibers were observed in cells plated on stiff substrates with the tress fibers mainly organized in the area of the cell located on top of the post. Similarly, in the case of soft silicone substrates, cells displayed more stress fibers toward the fragment of the cell located and attached on top of the micro-pattern.

These findings are for the most part consistent with previous reports. Literature has shown the cell cytoskeleton structure of the cell to play an important role in cell morphology,

cell differentiation and signal transduction (28). Previous reports have shown the actin cytoskeleton to be an important mediator between the cell and its extra-cellular environment (29). It has also been observed that the cells actin cytoskeleton structure is altered as a result of the presence of topography and variations in substrate stiffness (8, 30). In this study, the actin cytoskeleton structure was altered when seeded on PDMS substrates with varied stiffness. Furthermore, actin filaments were more pronounced at locations of the cell attached to the micro-patterns.

Numerous reports have investigated the effects of micro and nana-patterned surfaces on adipogenic differentiation. It has been reported that micro-grooves affect cell differentiation and alignment (9). A study showed the variation of nana-groove width to affect adipogenic differentiation. In addition, micro-pattern size and shape has also been shown to affect cell proliferation and differentiation (31). The depth of topographical patterns employed in studies has been shown to also affect cell behavior. However, there are few systematic studies which investigate multiple parameters of topography or multiple mechanical properties of the substrate simultaneously. This is necessary if our ultimate goal is to control cell differentiation, tissue regeneration, and viability of engineered constructs. It therefore seems essential for future studies to investigate variations of topographical pattern parameters in a single study. Future studies for this study may include varying pattern height, pitch, and size in order to see how adipogenic differentiation can be affected as a result of such changes. In order to fabricate polymer substrates with stiffness more representative of natural soft tissue, other synthetic or natural polymers could possibly be used as substrate models. Since it has been shown that pattern geometry alters stem cell

differentiation, future experiments can include fabrication of round posts in order to see if differentiation rate or percentage is affected by the geometry of such micro-patterned substrates.

The ultimate goal in tissue engineering is to control the microenvironmental niche in order to dictate stem cells differentiation into the desired cell types and ultimately guide tissue development. Both biochemical and biomechanical cues affect stem cell differentiation. Few studies have investigated multiple mechanical cues simultaneously. This study aimed to observe the effects of topographical cues and topographical stiffness on stem cell adipogenic differentiation using a pattern containing parameters both in the micron and sub micron range.

VI. CONCLUSION

The results of this study indicate that both mechanical and topographical cues may be introduced to manipulate stem cell responses. Adipogenic differentiation of hMSCs on patterned and non-patterned silicone substrates were compared. In addition, topographical stiffness effects on differentiation was also observed. There was a significant increase in differentiation when cells were cultured on patterned substrates at early time points. This increased rate of differentiation may have been as a result of initial aggregate formation and increased cell-cell contact in the presence of patterns with a 200 micron pitch. Observations were based on data obtained by detailed image analysis and quantitative analysis of lipid formation. In addition, actin cytoskeleton images show that cells do indeed respond to topographical patterns with varied stiffness. These results suggest that topography plays an important role in modulation of adipogenic differentiation. The results of this study may assist in the strategic design of in vitro models for soft tissue engineering applications.

VII. CITED LITERATURE

[1] Choi JH et al (2010) Adipose tissue engineering for soft tissue regeneration. Tissue Eng Part B Rev 16(4):413–426.

[2] American Society of Plastic Surgery. 2000/2010/2011 National Plastic Surgery Statistics. 2011.

[3] American Society of Plastic Surgery. 2000/2010/2011 National Reconstructive Plastic Surgery Statistics. 2011.

[4] Patrick, C.W., Jr., Chauvin, P.B., Robb, G.L.: Frontiers in Tissue Engineering, ed. C.W. Patrick, Jr., Mikes, A.G., McIntire, L.V., Oxford: Elsevier Science. 369-382, 1998.

[5] Bettinger C., Langer R., Borenstein J.: Engineering Substrate Topography at the Micro- and Nanoscale to Control Cell Function, Angew. Chem. Int Ed. 48:5406-5415, 2009.

[6] Discher, D. Engler, and A. Rehfeldt, F.: Cell responses to the mechanochemical microenvironment – implications for regenerative medicine and drug delivery, Advanced Drug Delivery Reviews 59(13):1329-1339, 2007.

[7] E. Martinez, E. Engel, et al.: Effects of artificial micro- and nano-structured surfaces on cell behavior. Annals of Anatomy 191:126-135, 2009.

[8] Liao H, Andersson AS, Sutherland D, Petronis S, Kasemo B, Thomsen P: Response of rat osteoblast-like cells to microstructured model surfaces in vitro. Biomaterials 24(4):649-654, 2003.

[9] Yam E., Pang S., Leong K.: Synthetic nanostructures inducing differentiation of human mesenchymal stem cells into neuronal lineage, Experimental Cell Research, 313:1820-1829, 2007.

[10] Chaubey et al.: Surface patterning: Tool to modulate Stem Cell Differentiation in an Adipose System. J Biomed Mater Res Part B: Appl Biomater 84B: 70–78, 2008.

[11] Von Heimburg, D., et al.: Human preadipocytes seeded on freeze-dried collagen scaffolds investigated in vitro and in vivo. Biomaterials 22(5): p. 429-38, 2002.

[12] Duranti, F., et al.: Injectable hyaluronic acid gel for soft tissue augmentation. A clinical and histological study. Dermatol Surg 24(12): p. 1317-25, 1998.

[13] Colter, D., et al.: Rapid expansion of recycling stem cells in cultures of plastic-Adherent cells from human bone marrow. Proc Natl Acad Sci 97:3213-3218, 2000.

[14] Kimura, Y., et al.: Adipose tissue engineering based on human preadipocytes combined with gelatin microspheres containing basic fibroblast growth factor. Biomaterials **24**(14): p. 2513-21, 2003.

[15] Minguell, J., et al.: Mesenchymal stem cells. Exp Biol Med 226: 507-520, 2001.

[16] Barry, F.: Biology and clinical applications of mesenchymal stem cells. Birth Defects Research 69: 250-256, 2003.

[17] Martin, G.: Isolation of pluripotent cell line from early mouse embryos cultured in medium conditioned by teratocarcinoma cells. Proc Natl Acad Sci USA 78:7634, 1981.

[18] Lutz, B.J.: Physicochemical Signals Direct Neuronal Differentiation of P19 Mouse Embryonal Carcinoma Cells. Master's Thesis, University of Illinois at Chicago, Illinois, 2009.

[19] Mehdizadeh, S.; Dukovic, J. O.; Andricacos, P. C.; Romankiw, L. T.; Cheh, H. Y.: The influence of lithographic patterning on current distribution: a model for microfabrication by electrodeposition. Journal of the Electrochemical Society 139(1): 78-91, 1992.

[20] Bilenberg, B.; Nielsen, T.; Clausen, B.; Kristensen A.: PMMA to SU-8 bonding for polymer based lab-on-a-chip systems with integrated optics. Journal of Micromechanics and Microengineering 14(6):814-818, 2004.

[21] Xia, Younan; Whitesides, George M. Soft lithography. Annual Review of Materials Science 28:153-184, 1998.

[22] Qin, Dong; Xia, Younan; Rogers, John A.: Jackman, Rebecca J.; Zhao, Xiao-Mei; Whitesides, George M. Microfabrication, microstructures and Microsystems. Topics in Current Chemistry 194:1-20, 1998.

[23] Maiellaro K.A.: Microfabricated Silicon Microchannels For Cell Rheology Study. Master's Thesis, University of Florida, Florida, 2003.

[24] Heinz WF, Hoh JH.: Spatially resolved force spectroscopy of biological surfaces using the atomic force microscope. Trends Biotechnol 17(4): 143-50, 1999.

[25] Alonso JL, Goldmann WH.: Feeling the forces: atomic force microscopy in cell biology. Life Sci 72(23): 2553-60, 2003.

[26] Titushkin I., and Cho M.: Modulation of cellular mechanics during osteogenic differentiation of human mesenchymal stem cells. Biophysical Journal 93:3693-702, 2007.

[27] Shenaq, S.M. and Yuksel E.: New research in breast reconstruction: adipose tissue engineering. Clin Plast Surg 29(1): p. 111-25, 2002.

[28] Bash D, Song L, Tuan RS.: Adult mesenchymal stem cells: Characterization, differentiation, and application in cell and gene therapy. J Cell Mol Med 8:301-16, 2004.

[29] S. R. Peyton, C. M. Ghajar, C. B. Khatiwala, and A. J. Putnam: The emergence of ECM mechanics and cytoskeletal tension as important regulators of cell function, Cell Biochemistry and Biophysics 47:300-320, 2007.

[30] Engler AJ, Sen S, Sweeney HL, Discher DE: Matrix elasticity directs stem cell lineage specification. Cell 126: 677–89, 2006.

[31] McBeath R, Pirone DM, Nelson CM, Bhadriraju K, Chen CS: Cell shape, cytoskeletal tension, and RhoA regulate stem cell lineage commitment. Dev Cell 6(4):483-495, 2004.

VITA

Hamed Naimipour

EDUCATION

University of Illinois at Chicago (UIC) - College of Engineering
MS in Bioengineering, GPA: 4.00, August 2012

University of Illinois at Chicago (UIC) - College of Engineering
BS in Bioengineering, GPA: 3.66, awarded May 2008, Graduated Cum Laude

RESEARCH EXPERIENCE

University of Illinois at Chicago (UIC), 8/10 – present
Graduate Student:

- Created PDMS replicas of a micro-patterned mask fabricated using training gained at the Nanotechnology core facility (NCF).
- Examined effects of substrate topology stiffness on stem cell behavior.
- Characterized substrate pattern dimensions using contact mode imaging of an atomic force Microscope.
- Characterized mechanical properties of cells taking force measurements using an atomic force microscope.

University of Illinois at Chicago (UIC), 8/09 – 8/10
Graduate Student:

- Familiarized with micro and nano-scale fabrication techniques.
- Gained training at the UIC nanotechnology core facility (NCF):
    - Learned methods of operation in a clean room setting along with operating a MJB3 mask aligner. Ultimately, a mask was designed, fabricated using photolithography, and used to create polymer scaffolds containing fabricated patterns.

University of Illinois at Chicago (UIC), 1/07 – 5/08
Undergraduate Research:

- Culturing and maintenance of mouse embryonic carcinoma stem cells and human mesenchymal stem cell lines.
- Collagen gel fabrication containing varied stiffness for controlled hMSC differentiation.
- Immunostaining and fluorescent staining of said stem cell lines for analysis of differentiation, calcium activity, and alterations in microfilament structure.

TEACHING EXPERIENCE

University of Illinois at Chicago (UIC), 1/11- 5/11
Teaching Assistant:

- Responsible for introduction and organization of guest lectures.
- Taught and reviewed various topics from micro-fabrication applications to stem cell applications in the context of tissue engineering.

University of Illinois at Chicago (UIC), 8/08 – 5/10
Teaching Assistant:

- Responsible for organizing and assigning teams with sponsored biomedical design projects.
- Corresponded with project leaders and the instructor regarding scheduled meetings between project sponsors and members.
- Monitored progress of teams and gave feedback regarding fallbacks and necessary adjustments related to the assigned project.

AWARDS & MEMBERSHIP

Graduate Student Council (GSC) Travel Award, UIC, AADR Conference, 2012.

Graduated Cum Laude, University of Illinois at Chicago

UIC, College of Engineering EXPO, *2nd Place Award* in Category of Medical Applications, Project Title: Mechanically-Directed Neurodifferentiation of Human Mesenchymal Stem Cells on Collagen Substrate, 2008

UIC College of Engineering Scholarship for academic excellence, 2006

Bio-Medical Engineering Society (BMES)

Dean/Donor Scholarship for academic excellence, 2005

Phi Kappa Phi (Top 10 percent of my class), Earned Status, 2008

Alpha Eta Mu Beta (AEMB), member, Fall 2006-2008